

# Force estimation in a 2-DoF piezoelectric actuator by using the inverse-dynamics based unknown input observer technique

Vincent TRENCHANT, Micky RAKOTONDRABE\* and Yassine HADDAB  
Automatic Control and MicroMechatronic Systems (AS2M) department  
FEMTO-ST Institute  
CNRS UMR-6174, University of Franche-Comté, ENSMM, UTBM  
24, rue Alain Savary Besançon France;  
corresponding author: mrakoton@femto-st.fr

## ABSTRACT

The aim of this paper is the estimation of force in a two degrees of freedom (2-DoF) piezoelectric actuator devoted to microrobotic manipulation tasks. Due to the limited space and to the small sizes of the actuator, the use of external sensors to measure both the displacement and the force played into role during the tasks are impossible. Therefore the deal in this study consists to propose observer techniques to bypass the use of force sensors. Based on the unknown input observer (UIO) technique, force along the two directions (y and z axes) of the actuator can be estimated precisely and with convenient dynamics. Additionally to the force, the state vector of the actuator is also estimated. Experimental tests are carried out and demonstrate the effectiveness of the method.

**Keywords:** Force estimation, 2-DoF piezoelectric actuator, unknown input observer, state and input estimation.

## 1. INTRODUCTION

Piezoelectric cantilever actuators are widely used as precise positioners thanks to their high bandwidth and high positioning resolution<sup>1-3</sup>. One of their principal applications in precise positioning is microrobotic tasks such as micromanipulation or microassembly<sup>3</sup>. Microrobotic tasks mainly involve real-time displacement measurement. However, knowing in real-time the force played into role potentially increases the performances and the success rate of the tasks. Measuring both the displacement and the force is however a great challenge in these applications due to the limited space and to the lack of performant but embeddable sensors to carry out the measurement. In fact, within the range of force played into role during a micromanipulation or a microassembly that we are dealt with (from  $1mN$  to tens of milliNewton)<sup>3,4</sup>, it is shown that there is a lack of convenient sensors. Indeed sensors that have the necessary performances in term of bandwidth, resolution and precision such as those based on capacitive sensors<sup>5</sup> are not embeddable and could not be used in real-time tasks situation. On the other hand, embeddable sensors like strain gage<sup>6</sup> do not often have the required performances, for instance in term of range or precision. It is also possible to equip a piezoelectric cantilevered actuator with an end-effector that has a force measurement feature, such as that presented in<sup>7,8</sup>. Based on silicon and piezoresistive materials, the end-effector was microfabricated in clean-room which may be costly and time-consuming. Finally, a promising work regarding the measurement of signals in a piezoelectric device working in microrobotic application consists to use the actuator as sensor at the same time. Called self-sensing<sup>9,10</sup>, this technique has an interesting packageability feature but requires a conveniently designed electrical circuit. To bypass the use of force sensors, a way consists in combining observer techniques with the available sensors, mostly displacement sensors, which permit to provide an estimate of the force in real-time thanks to mathematical algorithms. Observers present not only a packageability feature but also a low cost of the final device.

Observer techniques have been introduced as complementary measurement tools in piezoelectric actuators and proved their efficiency to track the force or the displacements with enough precision and/or enough bandwidth these last years. The challenge in estimating force is the fact that it is an exogenous signal in a piezoelectric

cantilevered actuator, and thus standard state estimation cannot be directly used. In addition, similarly to classically sized manipulators, micromanipulators such as piezoelectric cantilevered actuators have their force models strongly dependent on the manipulated objects characteristics <sup>12,13</sup>. In <sup>11</sup>, the force has still been considered as state and a Luenberger state-observer has been applied. To make the observer calculable, the force dynamics equation had to be imposed, which in this case was imposed equal to zero ( $\frac{dF}{dt} = 0$ ). In order to avoid the consideration of the force dynamics which needs to be modeled for every object manipulated, an inverse dynamics based force estimator (i.e. observer) was proposed in <sup>13</sup>. The aim consists in directly extracting the force from the initial model that links the input force, the input voltage, and the output displacement of the piezoelectric actuator. However since the estimation is 'open-loop', this technique is sensitive to model uncertainties. In addition, a direct inversion of the dynamics (transfer function) is carried out which requires some conditions on the model: bi-causality and non-minimum phase. Later on <sup>14</sup>, the force was considered as unknown input and then an unknown input observer (UIO) was applied. This approach has multiple advantages relative to the previous techniques: i) there is no need to have the force dynamics model, ii) the observer is 'closed-loop' (i.e. there is a real-time correction gain inside the observer) making this more robust than the open-loop estimation in <sup>13</sup>, iii) and the whole state of the actuator is also estimated additionally to the force. Furthermore, the UIO based force estimation can be combined with a self-sensing technology to have a fully packageable device where the force and the displacement measurements do not require external sensors <sup>15</sup>. Nonetheless, all these existing works were limited to single degree of freedom (1-DoF) piezoelectric actuators and are well convenient for monovarying force control <sup>16,17</sup>. They cannot be applied to multi-DoF actuators which are increasingly developed and used these last years <sup>18-23</sup>.

This paper deals with the estimation of force in a 2-DoF piezoelectric actuator. For that, the unknown input observer (UIO) based on inverse dynamics is proposed which permits to avoid the force dynamics modeling. Furthermore, the fact that the observer encloses a correction gain permits it to be more robust than 'open-loop' estimation technique. The main advance relative to the previous existing force estimation works in piezoelectric actuators is that we deal several degrees of freedom in this paper and the actuator exhibits strong cross-couplings that should be carefully modeled and accounted for in the observer synthesis. Experiments were carried out and demonstrated the efficiency of the approach.

The remainder of the paper is organized as follows. In section-2, we present the piezoelectric actuator and the experimental setup. Section-3 is devoted to the experimental modeling of the piezoelectric actuator and the parameters identification. The synthesis of the force observer as well as the experimental validation are developed in section-4. Finally, section-5 provides the conclusion of the paper.

## 2. PRESENTATION OF THE EXPERIMENTAL SETUP

The principle of the piezoelectric actuator used in this paper has been patented in <sup>22</sup> and employed as microrobotic device in <sup>24,25</sup>. Fig. 1 pictures the actuator used which has active dimensions of:  $22mm \times 1mm \times 0.9mm$ . It can perform a bending along two directions ( $y$  and  $z$  axes) thanks to two independent input voltages  $U_y$  and  $U_z$ . For each axis, the voltage input can range between  $\pm 10V$  and the output displacement between  $\pm 50\mu m$ . The whole experimental setup is composed of:

- the piezoelectric actuator (piezocantilever) itself,
- two displacement sensors used to measure the actuator bending along the  $y$  and  $z$  axes. The displacement sensors are inductive sensors from *IBS*-company and tuned to have in excess of  $1.5kHz$  of bandwidth which is sufficient for the experiments carried out,
- two force sensors from *femtools*-company used to measure the forces along the two axes. It is important to mention that these force sensors are only used to identify the model parameters and to validate the force observer technique proposed. Each of the two force sensors is mounted on a manual precise positioning table. Hence, it is possible to push the sensors towards the actuator permitting to simulate a manipulation force,

- a computer with Matlab-Simulink software which is used for to generate the voltages, to acquire the output signals (displacement, force) and to implement the observer. The sampling time is set equal to  $T_s = 50 \mu s$ . This is sufficiently small to account for the dynamics of the actuator and for the performances of the sensors,
- and a dSPACE-board which serves as interface between the computer and the external (sensors, actuator).

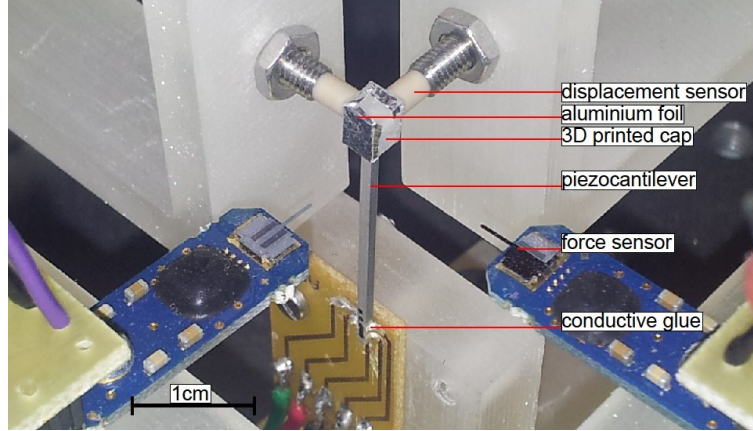


Figure 1: Presentation of the experimental setup.

### 3. MODELING THE 2-DOF PIEZOELECTRIC ACTUATOR

Let  $\delta = \begin{pmatrix} y \\ z \end{pmatrix}$  be the output displacement vector and let  $U = \begin{pmatrix} U_y \\ U_z \end{pmatrix}$  be the input voltage vector. Let also  $F = \begin{pmatrix} F_y \\ F_z \end{pmatrix}$  be the force vector that acts at the tip of the actuator. Assuming that the creep nonlinearity is neglectible, the relation that links the displacement  $\delta$  with the voltage  $U$  and the force  $F$  is given by <sup>25</sup>:

$$\delta(s) = \Gamma(U(s))D(s) - (s_p \circ D(s))F(s) \quad (1)$$

where  $s$  is the Laplace variable,  $\Gamma(U(s))$  is a rate-independent hysteresis operator,  $D(s)$  is a normalized dynamics ( $D_{ij}(s=0) = 1$ ,  $D_{ij}(s)$  being the elements of  $D(s)$ ) and  $s_p$  is the compliance of the actuator. Notation  $s_p \circ D(s)$  indicates the Hadamard product between the two matrices  $s_p$  and  $D(s)$ . We have:

$$D(s) = \begin{pmatrix} \frac{y}{U_y}(s) & \frac{y}{U_z}(s) \\ \frac{z}{U_y}(s) & \frac{z}{U_z}(s) \end{pmatrix} \quad (2)$$

where  $\frac{y}{U_y}$  and  $\frac{z}{U_z}$  stand for the dynamics in the direct transfers and  $\frac{y}{U_z}$  and  $\frac{z}{U_y}$  stand for the cross-couplings dynamics,

$$s_p = \begin{pmatrix} s_{pyy} & s_{pyz} \\ s_{pzy} & s_{pzz} \end{pmatrix} \quad (3)$$

where  $s_{pii}$  ( $i \in \{y, z\}$ ) indicate the direct transfers compliances, and  $s_{pij}$  ( $i \neq j$ ) indicate the cross-coupling compliances,

and

$$\Gamma(U(s)) = \begin{pmatrix} \Gamma_{yy}(U_y(s)) & \Gamma_{yz}(U_z(s)) \\ \Gamma_{zy}(U_y(s)) & \Gamma_{zz}(U_z(s)) \end{pmatrix} \quad (4)$$

where  $\Gamma_{ij}(U_j(s))$ , with  $i \in \{y, z\}$  and  $j \in \{y, z\}$ , is the hysteresis operator that links the output  $i$  with the input  $U_j$ . When  $i = j$ , we have the direct transfers, whilst when  $i \neq j$ , we have the cross-couplings.

### 3.1 Identification of the dynamics $D(s)$ parameters

To identify the dynamics  $D(s)$  parameters, step responses are used. First a step input voltage  $U_y$  of 5V amplitude is applied to the actuator whilst the voltage  $U_z$  is left equal to zero. The output displacement  $y$  is recorded and the direct transfer  $\frac{y}{U_y}$  is identified from the experimental data by using the ARMAX technique (Auto Regressive Moving Average with eXternal inputs) and the Matlab software <sup>26</sup>. In the meantime, the output displacement  $z$  is also recorded and the cross-coupling transfer  $\frac{z}{U_y}$  is identified. Afterwards, we set  $U_y = 0$  and apply a step voltage  $U_z = 5V$ . The resulting output  $y$  permits to identify the cross-coupling transfer  $\frac{y}{U_z}$  while the resulting output  $z$  permits to identify the direct transfer  $\frac{z}{U_z}$ . The identification yields:

$$D(s) = \begin{pmatrix} \frac{214.5s^2 + 1.147 \times 10^7 s + 1.633 \times 10^{11}}{s^3 + 2991s^2 + 1.02 \times 10^7 s + 2.957 \times 10^{10}} & \frac{-6.622s^2 - 3.29 \times 10^5 s - 3.732 \times 10^9}{s^3 + 1201s^2 + 1.018 \times 10^7 s + 1.147 \times 10^{10}} \\ \frac{253.4s^2 - 7.05 \times 10^5 s - 2.342 \times 10^8}{s^3 + 356.6s^2 + 1.01 \times 10^7 s + 3.283 \times 10^9} & \frac{332.3s^2 + 1.536 \times 10^7 s + 1.074 \times 10^{11}}{s^3 + 2802s^2 + 7.945 \times 10^6 s + 2.156 \times 10^{10}} \end{pmatrix}$$

(5)

Fig. 2 pictures the experimental step responses and the simulation of the identified model which shows a good adequacy, in particular for the direct transfers. Notice that the choice of the models orders during the identification was carried out as a compromise between the models simplicity and their precision.

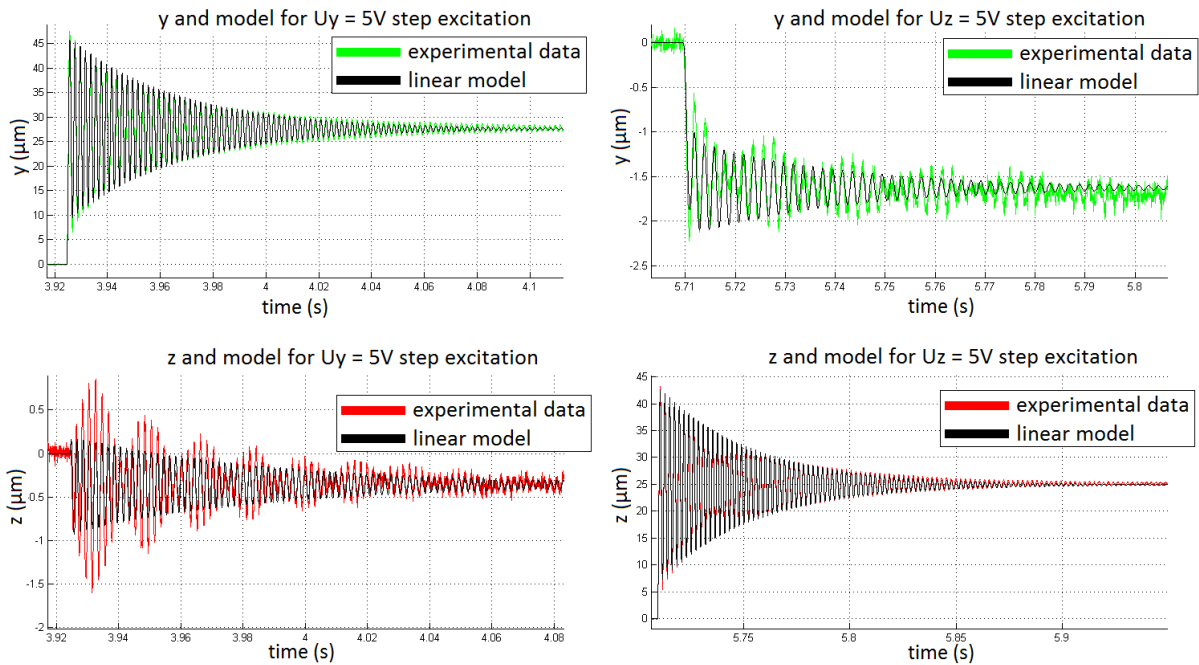


Figure 2: Experimental step responses and model simulation for the dynamics  $D(s)$ .

### 3.2 Identification of the hysteresis operator $\Gamma(U(s))$ parameters

There are several hysteresis modeling approaches used for smart materials, for instance: the Bouc-Wen approach <sup>27,28</sup>, the polynomial <sup>29</sup>, the lookup tables <sup>30</sup>, the Preisach <sup>31-36</sup>, the Phase-Preisach combined approach <sup>37</sup> and the Prandtl-Ishlinskii approach <sup>38-44</sup>. The classical Prandtl-Ishlinskii is based on the superposition of elementary operators called hysterons. It has an interesting precision feature and is well adapted to real-time applications. The hysteron in the classical Prandtl-Ishlinskii model is the play-operator or backlash. We choose this model for each of the transfer  $\Gamma_{ij}(U_j(s))$ . We first remind the backlash operator before presenting the classical Prandtl-Ishlinskii model. We shall use the time-domain notation  $\Gamma_{ij}(U_j(t))$  instead of the Laplace domain notation  $\Gamma_{ij}(U_j(s))$  for the hysteresis model.

A backlash (or play-operator)  $\gamma(U(t))$  is defined by:

$$s(t) = \gamma(U(t)) = \max \{U(t) - r, \min\{U(t) + r, \delta(t - T_s)\}\} \quad (6)$$

where  $T_s$  is the sampling time,  $r$  is the threshold,  $U$  is the input and  $s$  is the output of the backlash.

Thus, a complex hysteresis  $\Gamma_{ij}(U_j(t))$  is defined as the superposition of several backlashes:

$$\delta_i(t) = \Gamma_{ij}(U_j(t)) = \sum_{k=1}^{n_{ij}} w_{ijk} \cdot \gamma_{ijk} = \sum_{k=1}^{n_{ij}} w_{ijk} \cdot \max \{U_j(t) - r_{ijk}, \min \{U_j(t) + r_{ijk}, s_{ijk}(t - T_s)\}\} \quad (7)$$

where  $\delta_i \in \{y, z\}$  is the output, index  $ij$  stands for the transfer that links the input  $U_j$  with the output  $\delta_i$ ,  $n_{ij}$  is the number of backlashes in the model,  $w_{ijk}$  is the weighting of the  $k^{th}$  backlash,  $r_{ijk}$  is the threshold of this latter, and  $s_{ijk}$  is its elementary output.

The characterization of the hysteresis and identification of the model parameters are as follows. We first apply a sine input  $U_y$  with an amplitude of  $5V$  and a frequency of  $0.1Hz$  to the actuator,  $U_z$  being set equal to zero. We record the resulting output  $y$  and output  $z$ . Fig. 3-a (green) depicts the hysteresis of the direct transfer  $U_y \rightarrow y$  and Fig. 3-c (red) depicts that of the cross-coupling  $U_y \rightarrow z$ . Then we apply a sine input  $U_z$  with the same amplitude and frequency,  $U_y$  being set to zero. The resulting output  $y$  and output  $z$  permit to plot the cross-coupling  $U_z \rightarrow y$  (see Fig. 3-b (green)) and the direct transfer  $U_z \rightarrow z$  (see Fig. 3-z (red)) respectively. After imposing the number of backlashes  $n_{ij} = 15, \forall i$  and  $\forall j$ , the identification of the models parameters  $w_{ijk}$  and  $r_{ijk}$  follows the procedure in <sup>42</sup>. The simulation of the identified models is afterwards plotted in the same figures (see Fig. 3 (blue)) which well fits with the experimental hysteresis. Notice that the cross-couplings are almost linear.

### 3.3 Identification of the compliance $s_p$

The compliance  $s_p$  is identified as follows. First a constant force  $F_y$  is applied along the  $y$  axis by pushing the force sensor towards the actuator thanks to the manual precise positioning table. The resulting bending of the actuator along the two axes are measured and the compliances  $s_{pyy} = \frac{y}{F_y}$  and  $s_{pzy} = \frac{z}{F_y}$  are calculated. Then, the force  $F_y$  is set equal to zero and a force  $F_z$  is applied by pushing the second force sensor along the  $z$  axis towards the actuator. Then, with a similar way, the compliances  $s_{pyz} = \frac{y}{F_z}$  and  $s_{pzz} = \frac{z}{F_z}$  are calculated.

## 4. FORCE ESTIMATION USING THE UNKNOWN INPUT OBSERVER

We present in this section the estimation of the force  $F$ . The principle consists in considering the force as unknown input and in applying an unknown input observer to provide an estimate  $\hat{F}$ . An advantage of such structure is that there is no need to know the dynamics of the force which is strongly dependent on the manipulated object. In addition, the state of the actuator can also be estimated thanks to the observer.

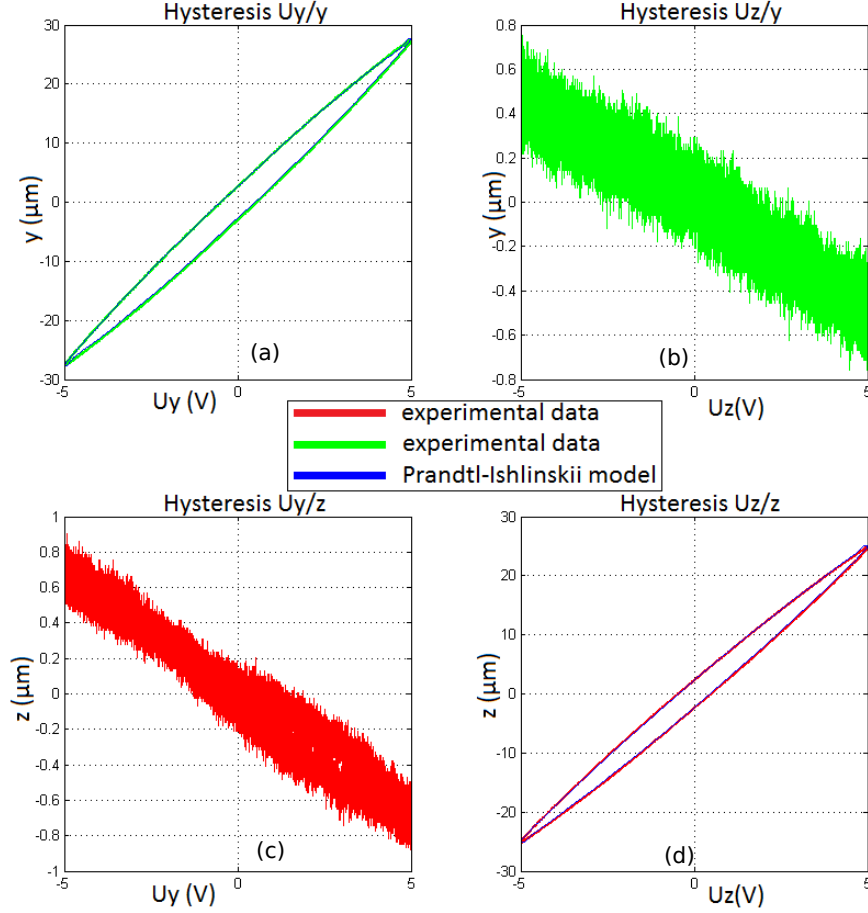


Figure 3: Experimental hysteresis and model simulation.

#### 4.1 Transforming into state-space representation

Let us first transform the model into a state-space representation. Applying similar way than for the monovariate case in <sup>14</sup>, the bivariable piezoelectric model in Eq. 1 can be transformed into state-space model as follows:

$$\begin{cases} \dot{x}(t) = Ax(t) + \beta(U(t), \delta(t)) + BF(t) \\ \delta(t) = Cx(t) \end{cases} \quad (8)$$

where  $x \in \mathbb{R}^{2n}$  is the state vector,  $\beta(U(t), \delta(t))$  is a nonlinear function including the effects of hysteresis,  $A \in \mathbb{R}^{2n \times 2n}$  is the state matrix,  $C \in \mathbb{R}^{2 \times 2n}$  is the output matrix and  $B \in \mathbb{R}^{2n \times 2}$  is the disturbance input matrix. The number  $n$  is the state number for the model of each axis. We have:  $n = 3$ .

#### 4.2 Observer principle

The UIO technique uses an estimation of the state of the system to generate an estimation of the unknown input (which is in our case the manipulation force). The UIO technique is therefore composed of two observers: a Luenberger observer which provides an estimate of the state, and the input observer which provides the estimate of the force. First, assume that the force  $F$  is known. Thus the Luenberger observer is described by:

$$\begin{cases} \dot{\hat{x}}(t) = A\hat{x}(t) + \beta(U(t), \delta(t)) + BF(t) + K(\delta(t) - \hat{\delta}(t)) \\ \hat{\delta}(t) = C\hat{x}(t) \end{cases} \quad (9)$$

where  $\hat{x}(t)$  is the estimate state,  $\hat{\delta}(t)$  is the estimate of the output displacement derived from  $\hat{x}(t)$ , and  $K$  is the state-observer gain which correct in real-time the estimation.

Then, based on the newly known signals, i.e. the input  $U(t)$ , the displacement  $\delta(t)$  and the estimate state  $\hat{x}(t)$  as well as its derivative  $\dot{\hat{x}}(t)$ , a force observer is constructed:

$$\hat{F}(t) = H_1\delta(t) + H_2\dot{\delta}(t) + G_1\hat{x}(t) + G_2\dot{\hat{x}}(t) + G_3\beta(U(t), \delta(t)) \quad (10)$$

where  $H_1$ ,  $H_2$ ,  $G_1$ ,  $G_2$  and  $G_3$  are the gains of the force observer.

The estimate force  $\hat{F}(t)$  is afterwards used for the state-observer in Eq. 9. Notice that in the force observer in Eq. 10, it is preferable to use the derivative  $\dot{\hat{\delta}}(t)$  of the estimate displacement instead of the derivative  $\dot{\delta}(t)$  of the measured displacement in order to avoid the amplification of noise. Based on these elements, the unknown input observer composed of Eq. 9 and Eq. 10 becomes:

$$\begin{cases} \dot{\hat{x}}(t) = A\hat{x}(t) + \beta(U(t), \delta(t)) + B\hat{F}(t) + K(\delta(t) - \hat{\delta}(t)) \\ \hat{\delta}(t) = C\hat{x}(t) \\ \hat{F}(t) = H_1\delta(t) + H_2\dot{\delta}(t) + G_1\hat{x}(t) + G_2\dot{\hat{x}}(t) + G_3\beta(U(t), \delta(t)) \end{cases} \quad (11)$$

The calculation of the state-observer gain  $K$  is based on the classical poles-assignment while the calculation of the force-observer gains  $H_1$ ,  $H_2$ ,  $G_1$ ,  $G_2$  and  $G_3$  is effectuated using the inverse dynamics technique in <sup>45</sup>.

Fig. 4 depicts the block-diagram of the UIO observer and of the piezoelectric actuator. As we can see, a filter  $\mathbb{F}(s)$  has been added inside the observer. This filter is used to avoid algebraic loop error that may occurs when the dynamics played into role is very quick, which is the case for piezoelectric systems. In order to not modify the functioning of the observer however, the filter is chosen to be as fast as possible. After different trials, the filter is chosen as:

$$\mathbb{F}(s) = \begin{pmatrix} \frac{1}{1+\tau_f s} & 0 \\ 0 & \frac{1}{1+\tau_f s} \end{pmatrix} \quad (12)$$

where  $\tau_f = T_s = 50\mu s$ .

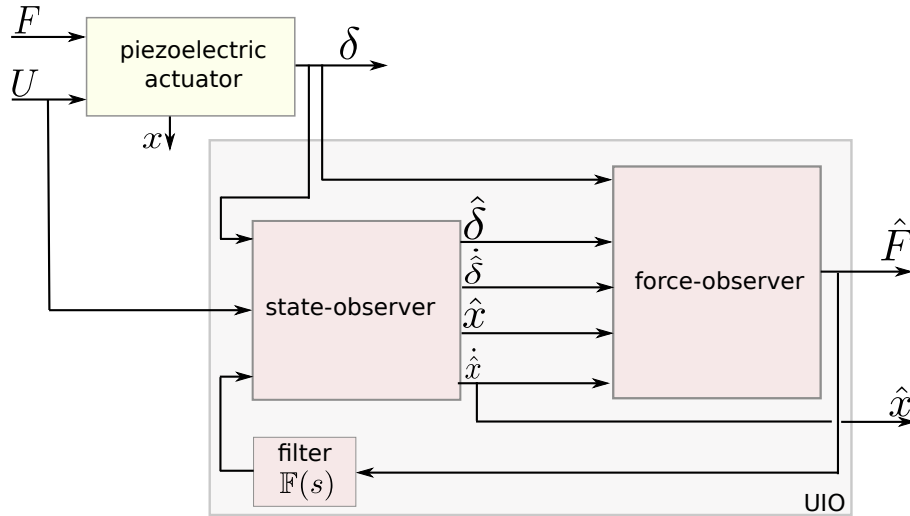


Figure 4: Structure of the unknown input observer.

### 4.3 Experimental results

The synthesized observer has been implemented in Matlab-Simulink and run in real-time thanks to the dSPACE board. To verify the efficiency of the observer, we carried out two experimental tests.

First, the estimation of a null force is carried out. For that, the force is left equal to zero:  $F = \begin{pmatrix} F_y \\ F_z \end{pmatrix} = \begin{pmatrix} 0 \\ 0 \end{pmatrix}$ . Then, we apply a series of steps of voltage  $U_y$  and  $U_z$ . Fig. 5-a depicts the resulting displacement along  $y$  axis (green) and along  $z$  axis (red) and Fig. 5-b depicts the estimate force  $\hat{F}_y$  (blue) and estimate force  $\hat{F}_z$  (black). As we can see from these results, whatever the displacements  $y$  and  $z$  are, the maximal error estimation in the force is  $0.8mN$  for  $F_y$  and  $0.55mN$  for  $F_z$ , except during the transient part where we can observe a peak in excess of  $1mN$  and of  $0.6mN$  respectively. These peaks are due to the uncertainties in the dynamics  $D(s)$  which therefore cause higher errors at high frequency.

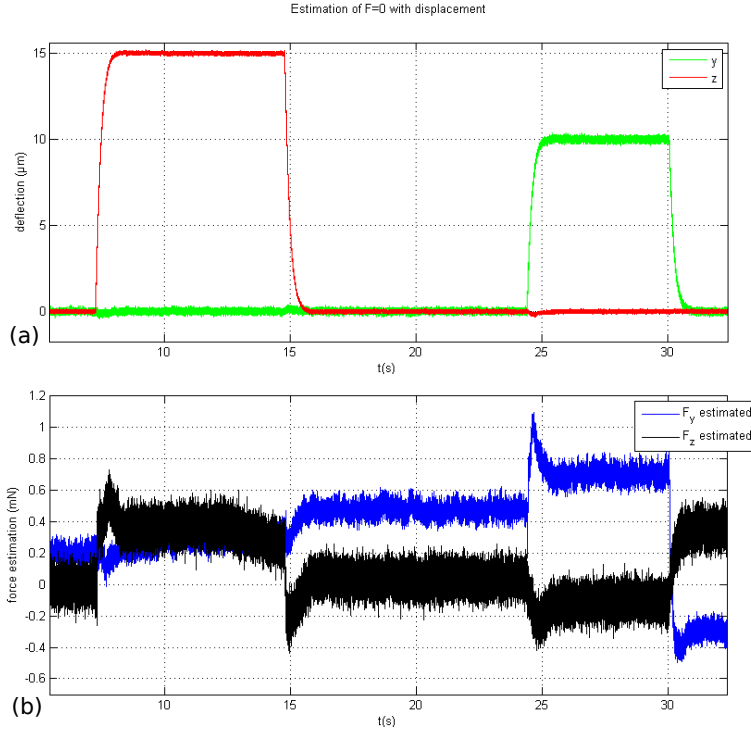


Figure 5: Estimation of a null-force.

We now leave the voltages  $U_y$  and  $U_z$  equal to zero and apply varying forces  $F_y$  and  $F_z$  by pushing the manual precise positioning tables that support the force sensors towards the actuator. In the meantime, the force sensors are used to measure the real force permitting to validate the estimates  $\hat{F}_y$  and  $\hat{F}_z$ . Fig. 6-a depicts the displacement  $y$  (green) when  $F_y$  is applied and Fig. 6-c depicts the corresponding force  $F_y$  (green) and the estimate force  $\hat{F}_y$  (blue). On the other hand, Fig. 6-b depicts the displacement  $z$  (red) when  $F_z$  is applied and Fig. 6-d depicts the corresponding force  $F_z$  (red) and the estimate force  $\hat{F}_y$  (black). These results clearly show that the estimate force  $F = \begin{pmatrix} \hat{F}_y \\ \hat{F}_z \end{pmatrix}$  well tracks the real force  $F = \begin{pmatrix} F_y \\ F_z \end{pmatrix}$  which demonstrate the efficiency of the observer even in presence of the hysteresis nonlinearity and of the strong cross-couplings that typify the actuator.

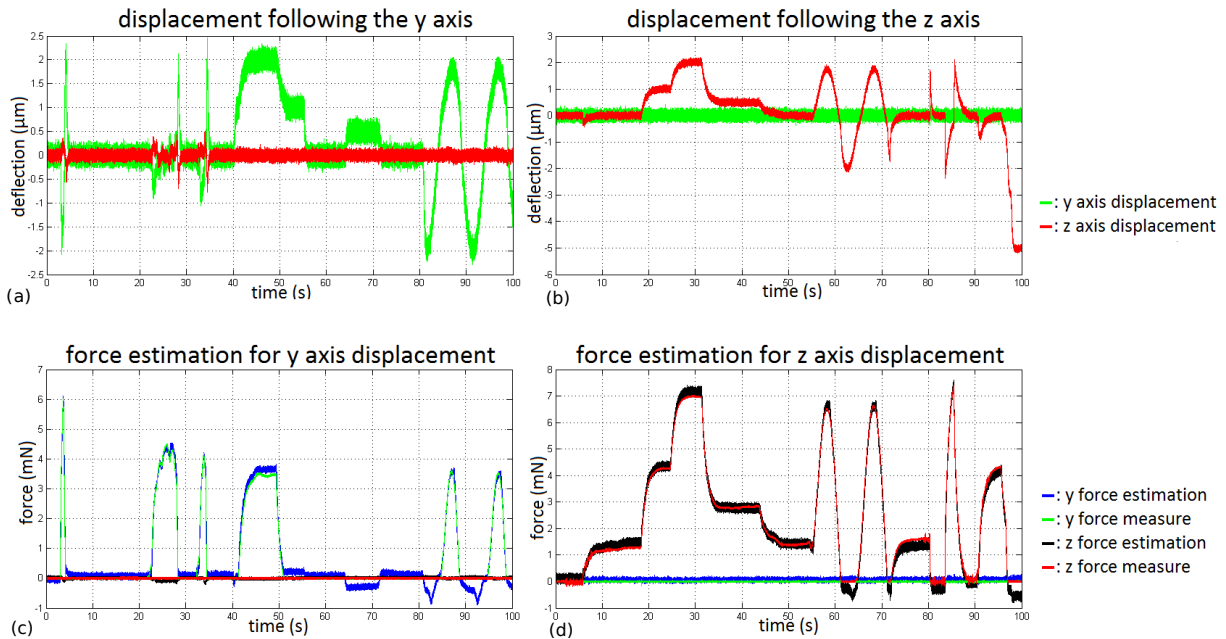


Figure 6: Estimation of a non-null force.

## 5. CONCLUSIONS

This paper presented the estimation of the force in a piezoelectric cantilever actuator. The actuator has two degrees of freedom (2-DoF) and the force to be estimated is along two axes. Furthermore, the actuator exhibits hysteresis nonlinearities and strong cross-couplings to be accounted for. For all that, we proposed to use an unknown input observer which permitted to provide an estimate of the force without knowing its dynamics. The observer also permitted to provide an estimate of the full state of the actuator. Experimental tests were carried out and confirmed the efficiency of the approach. As future works, the results in this paper will be implemented for real-time micromanipulation tasks based on piezoelectric microgripper and with force and position control strategy.

## Aknowledgments

This work is supported by the national ANR-JCJC C- MUMS-project (National young investigator project ANR-12- JS03007.01: Control of Multivariable Piezoelectric Microsystems with Minimization of Sensors). This work is also supported by the LABEX ACTION.

## REFERENCES

- [1] J. L. Pons, "Emerging actuator technology: a micromechatronic approach", Wiley, ISBN: 0-470-09197-5, 2005.
- [2] S. Devasia, E. E. Eleftheriou, R. Moheimani, "A survey of control issues in nanopositioning", IEEE Transactions on Control Systems Technology, Vol.15, N<sup>o</sup>15, pp.802-823, 2007.
- [3] J. Agnus, N. Chaillet, C. Clévy, S. Dembélé, M. Gauthier, Y. Haddab, G. Laurent, P. Lutz, N. Piat, K. Rabenorosoa, M. Rakotondrabe and B. Tamadazte, 'Robotic Microassembly and micromanipulation at FEMTO-ST', Journal of Micro-Bio Robotics (JMBR), Volume 8, Issue 2, Page 91-106, 2013.
- [4] C. Clévy, M. Rakotondrabe and N. Chaillet, 'Signal measurement and estimation techniques issues in the micro/nano world', edited book, Springer - Verlag, New York, ISBN 978-1-4419-9945-0, August 2011.
- [5] The femtotools company: <http://www.femtotools.com/>.
- [6] M. Boudaoud and S. Régnier, 'An overview on gripping force measurement at the micro and nano-scales using two-fingers microrobotic systems', International Journal of Advanced Robotic Systems, doi: 10.5772/57571, 2014.

- [7] J. Agnus, 'Sensorized silicone finger tip', french patent 2010.
- [8] X. Xu, J. Agnus and M. Rakotondrabe, 'Development and characterization of a new silicone/platine based 2-DoF sensorized end-effector for micromanipulators', SPIE - Sensing Technology+Applications; Sensors for Next Generation Robots conference , 911608, doi: 10.1117/12.2049041, Baltimore Maryland USA, May 2014.
- [9] A. Ivan, M. Rakotondrabe, P. Lutz and N. Chaillet, 'Current integration force and displacement self-sensing method for cantilevered piezoelectric actuators', Review of Scientific Instruments (RSI), Vol.80(12), 2126103, December 2009.
- [10] M. Rakotondrabe, A. Ivan, S. Khadraoui, P. Lutz and N. Chaillet, 'Simultaneous displacement and force self-sensing in piezoelectric actuators and applications to robust control of the displacement', IEEE/ASME - Transactions on Mechatronics (T-mech), Vol 20No 2, Page 519 - 531, April 2015.
- [11] Y. Haddab, "Conception et réalisation d'un système de micromanipulation contrôlé en effort et en position pour la manipulation d'objets de taille micrométrique", PhD Thesis (in french), Franche-Comté University, France, 2000.
- [12] S. D. Eppinger and W. P. Seering, 'On dynamic models of robot force control', International Conference on Robotics and Automation, IEEE ICRA, April 1986.
- [13] M. Rakotondrabe, Y. Haddab and P. Lutz, 'Nonlinear modelling and estimation of force in a piezoelectric cantilever', IEEE/ASME International Conference on Advanced Intelligent Mechatronics, Zurich Switzerland, Sept 2007.
- [14] M. Rakotondrabe and P. Lutz, 'Force estimation in a piezoelectric cantilever using the inverse-dynamics-based UIO technique', IEEE International Conference on Robotics and Automation, pp:2205-2210, Kobe Japan, May 2009.
- [15] M. Rakotondrabe, 'Combining self-sensing with an Unknown-Input-Observer to estimate the displacement, the force and the state in piezoelectric cantilevered actuator', ACC, (American Control Conference), pp.4523-4530, Washington DC USA, June 2013.
- [16] M. Rakotondrabe, Y. Haddab and P. Lutz, 'Modelling and H-inf force control of a nonlinear piezoelectric cantilever', IEEE/RSJ - IROS, (International Conference on Intelligent Robots and Systems), pp:3131-3136, San Diego CA USA, Oct-Nov 2007.
- [17] M. Rakotondrabe and Y. Le Gorrec, 'Force control in piezoelectric microactuators using self scheduled H-inf technique', IFAC - Mech, (Symposium on Mechatronic Systems), pp.417:422, Cambridge Massachusetts USA, September 2010.
- [18] G. Binnig, C. F. Quate, Ch. Gerber, "Atomic Force Microscope". Physical Review Letters 56 (9): 930-933, 1986.
- [19] M. Rakotondrabe, Y. Haddab and P. Lutz, 'Design, development and experiments of a high stroke-precision 2DoF (linear-angular) microsystem', IEEE International Conference on Robotics and Automation, pp:669-674, Orlando FL USA, May 2006.
- [20] B. J. Kenton, K. K. Leang, "Design and control of a three-axis serial-kinematic high-bandwidth nanopositioner", IEEE/ASME Trans. Mechatronics, 17 (2), pp. 356 à 369, 2012.
- [21] W. Liao, W. Liu, Y. Zhu, Y. Tang, B. Wang, and H. Xi, 'A Tip-Tilt-Piston Micromirror With Symmetrical Lateral-Shift-Free Piezoelectric Actuators', IEEE Sensors Journal, 13(8), pp. 2873-2881, 2013.
- [22] J. Agnus, P. De Lit and N. Chaillet, 'Micromanipulateur piézoélectrique notamment pour microrobotique', french patent, FR0211934, 2002.
- [23] A. Bienaimé, V. Chalvet, C. Clévy, L. Manuel-Gauthier, T. Baron and M. Rakotondrabe, 'Static / dynamic trade-off performance of PZT thickfilm micro-actuators', IOP - Journal of Micromechanics and Microengineering (JMM), under publication, 2015.
- [24] M. Rakotondrabe, J. Agnus and P. Lutz, 'Feedforward and IMC-feedback control of a nonlinear 2-DOF piezoactuator dedicated to automated micropositioning tasks', IEEE - CASE, (International Conference on Automation Science and Engineering), pp.393-398, Trieste Italy, August 2011.
- [25] M. Rakotondrabe, 'Smart materials-based actuators at the micro/nano-scale: characterization, control and applications', edited book, Springer - Verlag, New York, ISBN 978-1-4614-6683-3, 2013.
- [26] L. Ljung, 'System identification toolbox', The Matlab user's guide.

- [27] M. Rakotondrabe, 'Bouc-Wen modeling and inverse multiplicative structure to compensate hysteresis non-linearity in piezoelectric actuators', IEEE Transactions on Automation Science and Engineering, Vol.8(2), pages 428-431, April 2011.
- [28] D. Habineza, M. Rakotondrabe and Y. Le Gorrec, 'Bouc-Wen Modeling and Feedforward Control of multi-variable Hysteresis in Piezoelectric Systems: Application to a 3-DoF Piezotube scanner', IEEE Transactions on Control Systems Technology, DOI.10.1109/TCST.2014.2386779.
- [29] S. Bashash and N. Jalili, 'A Polynomial-Based Linear Mapping Strategy for Feedforward Compensation of Hysteresis in Piezoelectric Actuators', ASME Journal of Dynamic Systems, Measurement and Control, Vol.130(3), 10 pages, DOI.10.1115/1.2907372, May 2008.
- [30] K. Kyle Eddy, 'Actuator bias prediction using lookup-table hysteresis modeling', US Patent-08/846545, February 1999.
- [31] D. Croft, G. Shed and S. Devasia, 'Creep, hysteresis and vibration compensation for piezoactuators: atomic force microscopy application', ASME Journal of Dynamic Systems, Measurement and Control, Vol.123(1), pages 35-43, March 2001.
- [32] A. Dubra and J. Massa and C.l Paterson, 'Preisach classical and nonlinear modeling of hysteresis in piezo-ceramic deformable mirrors', Optics Express, Vol.13(22), pages 9062-9070, 2005.
- [33] X. Tan and J. S. Baras, 'Modeling and control of hysteresis in magnetostrictive actuators,' Automatica, vol.40(9), pages 1469-1480, 2004.
- [34] R. V. Iyer, X. Tan and P. S. Krishnaprasad, 'Approximate Inversion of the Preisach Hysteresis Operator With Application to Control of Smart Actuators', IEEE Transactions on Automatic Control, pages 798-810, Vol.50(6), June 2005.
- [35] D. Hughes and J. T. Wen, 'Preisach modeling and compensation for smart material hysteresis,' Active Materials and Smart Structures, vol.2427, pages.50-64, 1994.
- [36] S. Mittal, C.H Menq, "Hysteresis compensation in electromagnetic actuators through Preisach model inversion", IEEE/ASME Transactions on Mechatronics, vol.5(4), pages.394-409, 2000.
- [37] J. Manuel Cruz-Hernandez and V. Hayward, 'Phase Control Approach to Hysteresis Reduction', IEEE Transactions on Control Systems Technology, Vol.9(1), January 2001.
- [38] W. T. Ang, P. K. Kholsa and C. N. Riviere, 'Feedforward controller with inverse rate-dependent model for piezoelectric actuators in trajectory-tracking applications', IEEE/ASME Transactions on Mechatronics, Vol.12(2), pages 134-142, April 2007.
- [39] B. Mokaberi and A. A. G. Requicha, 'Compensation of scanner creep and hysteresis for AFM nanomanipulation', IEEE Transactions on Automation Science and Engineering, Vol.5(2), pages 197-208, April 2008.
- [40] K. Kuhnen and H. Janocha, 'Inverse feedforwad controller for complex hysteretic nonlinearities in smart-materials systems', Control of Intelligent System, Vol.29(3), 2001.
- [41] M. Al Janaideh, S. Rakheja, C. Y. Su, 'An analytical generalized Prandtl-Ishlinskii model inversion for hysteresis compensation in micropositioning control', IEEE/ASME on Transactions Mechatronics, Vol.16(4), 734-744
- [42] M. Rakotondrabe, 'Classical Prandtl-Ishlinskii modeling and inverse multiplicative structure to compensate hysteresis in piezoactuators', American Control Conference, pages 1646-1651, Montréal Canada, June 2012.
- [43] X. Liu, Y. Wang, J. Geng and Z. Chen, "Modeling of hystersis in piezoelectric actuator based on adaptive filter," Sensors and Actuators A: Physical, vol.189, pp.420-428, 2013.
- [44] U.X. Tan, W.T. Latt, F. Widjaja, C.Y. Shee, C.N. Riviere and W.T. Ang, "Tracking Control of Hysteretic Piezoelectric Actuator using Adaptive Rate-Dependent Controller," Sensors and Actuators A: Physical, vol.150, pp.116-123, 2009.
- [45] C-S. Liu and H. Peng, 'Inverse-dynamics based state and disturbance observers for linear time-invariant systems', ASME Journal of Dynamics Systems, Measurement and Control, vol.124, pp.375-381, September 2002.